









Origin of the Weak Plasma Emission Line Detected by Voyager 1 in the Interstellar Medium: Evidence for Suprathermal Electrons

D. A. Gurnett¹ , W. S. Kurth¹ , L. F. Burlaga² , D. B. Berdichevsky^{3,4}, N. V. Pogorelov⁵ , M. Pulupa⁶ , and S. D. Bale^{6,7} 

¹Univ. of Iowa, Dept. of Physics and Astronomy, Iowa City, IA 52242, USA; donald-gurnett@uiowa.edu

²Leonard F. Burlaga, Inc., Davidsonville, MD 21035, USA

³IFIR/CONICET-UNR, Esmeralda y 27 de Febrero, Rosario, Santa Fe, Argentina

⁴Trident-Berdichevsky, Daniel B. Partnership, Greenbelt, MD 20771, USA

⁵Univ. of Alabama, Dept. of Space Science, Huntsville, AL 35805, USA

⁶Univ. of California/Berkeley, Space Sciences Laboratory, Berkeley, CA 94720, USA

⁷Univ. of California/Berkeley, Physics Dept., Berkeley, CA 94720, USA

Received 2021 June 24; accepted 2021 August 6; published 2021 November 1

Abstract

Recently, a very weak, nearly continuous plasma wave emission line has been discovered in the nearby interstellar medium at the electron plasma frequency. The new observations were made by the plasma wave instrument on the Voyager 1 spacecraft, which crossed into the interstellar medium in 2012 August. Several questions remained unanswered after the initial discovery. Why was the emission line not observed until several years after Voyager 1 entered the interstellar medium, what is the wavelength of the plasma oscillations responsible for the emission line, and what is the origin of the oscillations? Here, we provide answers to these questions. On the most important question, namely the origin of the oscillations, the evidence strongly suggest that the emission is driven by suprathermal electrons that excite plasma oscillations comparable to the quasi-thermal noise (QTN) that is commonly observed by space plasma wave instruments with long, thin electric dipole antennas. These results imply the existence of a relatively dense population of suprathermal electrons that could contribute significantly to the overall pressure in the interstellar medium. Although the similarities to the previous QTN observations are impressive, there is no certainty that the emissions are driven by thermal excitation, and other sources should be explored, such as the possibility that they are driven by pressure fluctuations associated with the short-wavelength cascade of interstellar turbulence.

Unified Astronomy Thesaurus concepts: [Interstellar plasma \(851\)](#)

1. Introduction

The Voyager 1 and 2 spacecraft crossed the heliopause into the very local interstellar medium (VLISM) in 2012 and 2018, respectively (Burlaga et al. 2013, 2019; Gurnett et al. 2013; Krimigis et al. 2013, 2019; Stone et al. 2013, 2019; Gurnett & Kurth 2019; Richardson et al. 2019). The heliopause is the boundary (Davis 1955; Parker 1963; Axford 1990; Zank 2015) between the hot, 10^5 – 10^6 K (McComas et al. 2011), plasma flowing outward from the Sun and the relatively cold, $\sim 10^4$ K (Frisch et al. 2011), plasma in the VLISM. Since then, the plasma wave science (PWS) instruments on both Voyagers 1 and 2 have been providing electron densities from the frequencies of electron plasma oscillations observed in the interstellar plasma (Gurnett & Kurth 2019). The plasma oscillations are driven by upstream electron beams from shocks propagating outward from the Sun, comparable to plasma oscillations generated by electron beams upstream of Earth’s bow shock (Filbert & Kellogg 1979). However, recently Ocker et al. (2021) discovered a very weak plasma emission line at the electron plasma frequency that often extends smoothly between the upstream shock-driven electron plasma oscillations. When present, this plasma wave emission line provides continuous measurements of the local electron density, a significant advance in our ability to study short-term density variations in the VLISM, such as the pressure fronts reported by Burlaga et al. (2021). Here, we address several important questions regarding the newly discovered plasma wave emissions. Specifically, we comment on why the emission line was not observed before about 2016, on the wavelengths of the emissions, and on their likely origin.

2. Why Are the Emissions Not Observed before About 2016?

A frequency–time spectrogram of electron plasma oscillations detected by the Voyager 1 PWS wideband waveform receiver is shown in Figure 1. This spectrogram covers the period from shortly before the heliopause crossing in 2012 to the most recent data in 2020. The events indicated by the red arrows labeled “Shock-Driven Upstream Electron Plasma Oscillations” are the very intense electron plasma oscillations driven by electron beams from shocks propagating outward from energetic solar events. The newly discovered very weak emission line extending nearly continuously between the shock-driven plasma oscillations is indicated by the orange arrows labeled “Continuous Plasma Emission Line.” As can be seen, the frequency of this emission line closely matches the frequencies of the shock-driven emissions, which have earlier been identified as being at the electron plasma frequency (Gurnett et al. 2013). The electron plasma frequency is given by $f_p = 8980\sqrt{n_e}$ Hz (Gurnett & Bhattacharjee 2017), where n_e is the electron density in cm^{-3} . The corresponding electron densities are shown by the scale on the right-hand side of the spectrogram.

Careful inspection of Figure 1 shows that there is no evidence of the newly discovered plasma emission line before about 2016. The question then arises, why were the emissions not observed before about 2016? Since electron plasma oscillations are a normal mode of the plasma in which the electrons move freely along the static magnetic field, the electric field of these oscillations is aligned in the direction of the static magnetic field

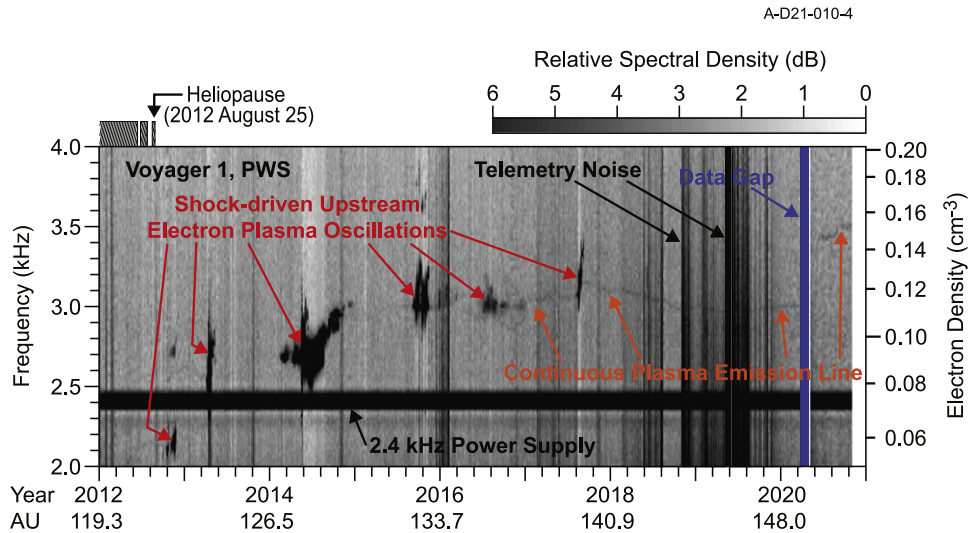


Figure 1. A frequency–time spectrogram of the electric field waveforms detected by the Voyager 1 plasma wave instrument from shortly before the heliopause crossing in 2012 August to the latest data in 2020, adapted from Burlaga et al. (2021). The heliopause is the boundary (Davis 1955; Parker 1963; Axford 1990; Zank 2015) between the hot solar wind plasma in the heliosphere, and the relatively cold interstellar plasma. The electron densities given by the frequency of the plasma oscillations are shown by the scale on the right side of the spectrogram.

(Gurnett et al. 2013). Given this constraint, we have considered whether long-term variations of the interstellar magnetic field direction with respect to the electric antenna axis could account for the absence of the plasma wave emission line before about 2016. The PWS electric antenna consists of two 10 m elements oriented in a 90° V-shaped configuration on the spacecraft as shown in Figure 2. The PWS uses these two elements as an electric dipole antenna, which means that the receiver responds to the voltage difference between the centers of the two elements. From the geometry, it follows that the effective axis of the PWS electric antenna is oriented parallel to the x -axis of the spacecraft. The amplitude of the voltage signal is then proportional to the absolute value of $\cos \alpha$, where α is the angle between the magnetic field direction and the spacecraft x -axis. To explore long-term variations, we used measurements from the spacecraft magnetometer (MAG) to determine variations of the angle α . The results are shown in Figure 3. The top panel shows that the angle α decreased from about 27° shortly after the heliopause crossing to about 10° in the most recent data. Since $\alpha = 0^\circ$ represents perfect alignment, any deviation from $\alpha = 0^\circ$ constitutes a loss of signal power. This loss is given by $20 \log_{10}(|\cos \alpha|)$ in dB and is shown in the bottom panel of Figure 3. As can be seen, the loss decreases systematically from near the heliopause to near zero in the most recent data. Although this loss of signal power is small, only about 1 dB, the signal-to-noise ratio of the plasma emission line is also small, only about 1 dB above the prevailing noise background (Ocker et al. 2021). Based on these comparisons, we conclude that the systematic change in the interstellar magnetic field direction relative to the effective axis of the PWS electric antenna explains why the plasma wave emission line was not observed before about 2016. Note the rapid improvement in the alignment of the magnetic field direction relative to the antenna beginning in 2015, which corresponds well with the increasing strength of the emission line from 2015 to 2017 (see Figure 1).

3. Wavelengths of the Emissions

In a cold plasma, the frequency of electron plasma oscillations is constant, completely independent of wavelength. However, if the electrons have a nonzero temperature, as in the

VLISM, the electron pressure acts to increase the frequency of the oscillations. When electron pressure effects are included, the dispersion relation of electron plasma oscillations is given by the Langmuir wave dispersion relation (Tonks & Langmuir 1929):

$$\omega^2 = \omega_p^2 [1 + 3\lambda_D k^2], \quad (1)$$

where λ_D is the Debye length, $k = 2\pi/\lambda$ is the wavenumber, and λ is the wavelength. The Debye length is given by $\lambda_D = 6.9(T_e/n_e)^{1/2}$ cm, where T_e is the electron temperature in K, and the electron velocity distribution is assumed to be a Maxwellian. Electron plasma oscillations are often called Langmuir waves. However, here we call them simply electron plasma oscillations. Equation (1) is only valid for wavelengths substantially greater than the Debye length, because strong Landau damping occurs when the wavelength is comparable to, or less than, the Debye length (Gurnett & Bhattacharjee 2017). Note that the wavelength decreases as the oscillation frequency increases. This inverse dependence of the oscillation frequency on the wavelength implies that the bandwidth of the emission line should increase as the wavelength decreases.

To use the observed bandwidth of the emission line, $\Delta\omega$, to investigate the wavelengths involved in the oscillations, we assume that the emission line extends from a lower frequency limit of $\omega = \omega_p$, where the wavelength is infinite ($k = 0$), to an upper frequency limit, $\omega = \omega_p + \Delta\omega$, where the wavelength is a minimum, given by $\lambda_{\min} = 2\pi/k$. By expanding the dispersion relation around $k = 0$ and using $\omega = \omega_p + \Delta\omega$, it is easy to show that the minimum wavelength, λ_{\min} , is given by

$$\lambda_{\min} = 2\pi \sqrt{\frac{3}{2}} \lambda_D Q^{1/2}, \quad (2)$$

where the factor $Q = \omega_p/\Delta\omega$ is a qualitative measure of the sharpness of the emission line. It is obvious from Figure 1 that the bandwidth of the plasma emission line is extremely narrow, which implies a large Q . Specifically, Ocker et al. (2021) report a bandwidth of $\Delta f = 40$ Hz at a typical oscillation frequency of

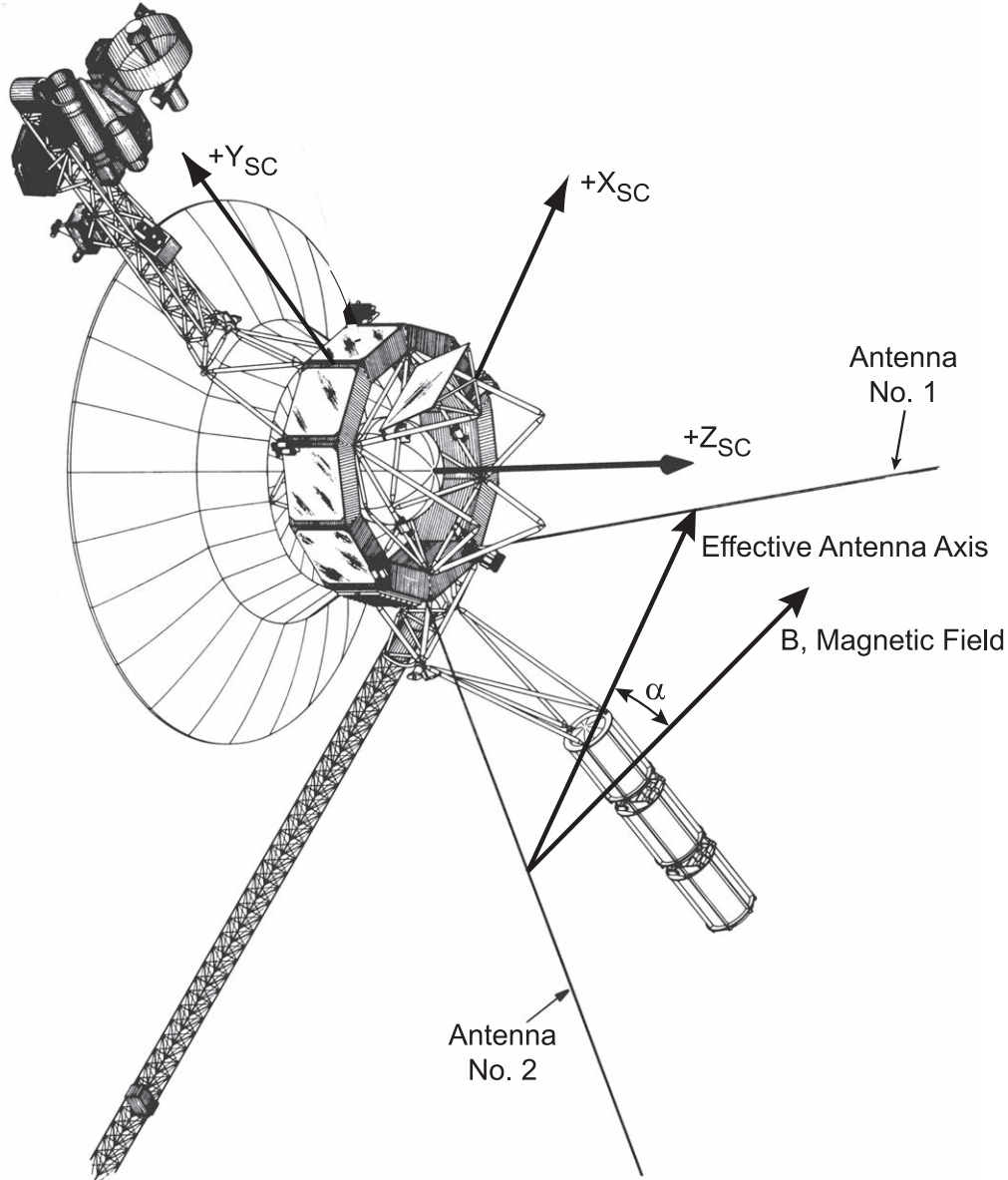


Figure 2. The Voyager PWS plasma wave electric antenna consists of two 10 m elements mounted on the spacecraft in a 90 K V-shaped configuration and is operated as a dipole by measuring the voltage difference between the centers of the two elements. The effective axis of the dipole is parallel to the x -axis of the spacecraft and has an effective length of 7.1 m. The interstellar magnetic field is measured by the spacecraft magnetometer and is at an angle α with respect to the effective axis of the dipole.

$f_p = 3000$ Hz, which gives $Q = 75$. Using an electron temperature of $T_e = 30,000$ K, as estimated from measurements by the plasma instrument (PLS) on Voyager 2, and a typical electron density of $n_e = 0.12 \text{ cm}^{-3}$, as determined from plasma oscillation frequency measurements by the Voyager 1 PWS, the Debye length is found to be $\lambda_D = 35$ m. Equation (2) then gives a minimum wavelength of $\lambda_{\min} = 2.3$ km. This minimum wavelength implies that the wavelength of most of the waves are rather long, on the order of kilometers or more, much longer than the 7.1 m effective length of the PWS dipole antenna. It also implies that the phase velocities of the waves, λ_f , are rather large, 3000 km s^{-1} or more, substantially greater than the electron thermal velocity, which is 1170 km s^{-1} for 30,000 K.

Another factor potentially affecting the observed bandwidth of the emission line is the Doppler spreading caused by the rapid flow of the VLISM plasma past the spacecraft. If there is a broad range of wavelengths involved, as would be expected for oscillations driven by thermal or turbulent fluctuations, Doppler shifts act to broaden the frequency spectrum of the emission line. From ultraviolet measurements, it is known that the interstellar plasma is flowing toward the Sun at a speed of about 26 km s^{-1} (Ajello et al. 1987). Voyager 1 is also moving somewhat northward out of the ecliptic plane, toward the nose of the heliosphere, at a speed of about 16 km s^{-1} . Considering the angle between the spacecraft velocity vector and the direction of the interstellar plasma flow, we estimated that the flow velocity of the interstellar plasma relative to the spacecraft is about $v = 41 \text{ km s}^{-1}$. To calculate the resulting Doppler shift, one must

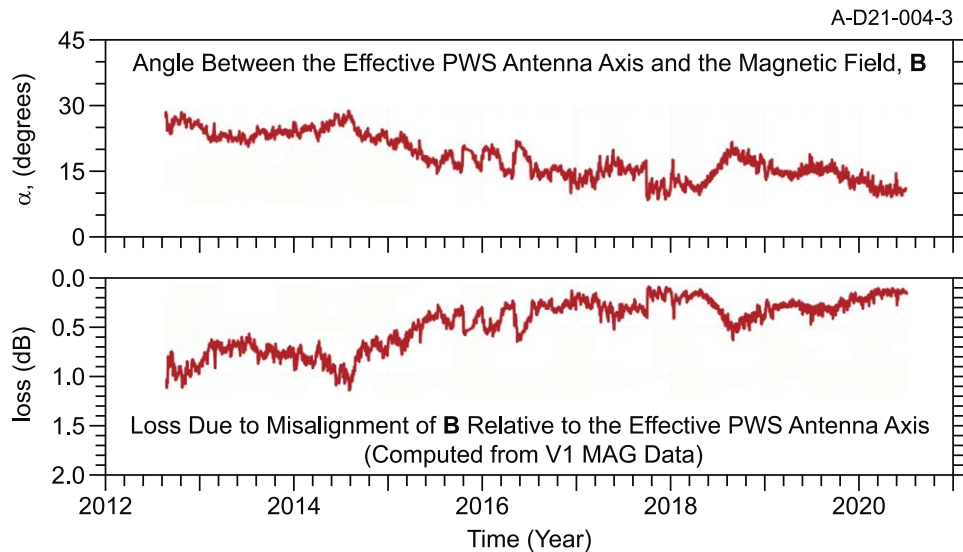


Figure 3. Since the electric field of electron plasma oscillations is always parallel to the static magnetic field, the voltage detected by the PWS electric antenna is proportional to the cosine of the angle α between the effective axis of the antenna and the magnetic field. The top panel shows the long-term variations of α as a function of time, and the bottom plot shows the resulting loss, in dB, of the antenna response relative to perfect, $\alpha = 0^\circ$, alignment. This loss decreased by about 1 dB from shortly after the heliopause crossing to the most recent data. This variation is believed to be responsible for the fact that the plasma emission line in Figure 1 could not be detect before about 2016.

consider the relative angle between the \mathbf{k} vector of the plasma oscillations (which we assume is along \mathbf{B}) and the interstellar plasma flow velocity \mathbf{v} . Using the results of Ajello et al. (1987) and models of the interstellar plasma flow around the heliosphere (Kim et al. 2017; Pogorelov et al. 2017), we estimate the angle between \mathbf{k} and \mathbf{v} is about $\theta_{kv} = 110^\circ$. From the equation for the Doppler shift, $\Delta\omega = kv \cos \theta_{kv}$, and assuming that the waves are likely to be propagating in both directions along the magnetic field, the resulting Doppler spread is given approximately by $\Delta f = (2v/\lambda_{\min}) \cos \theta_{kv}$. From the measured bandwidth of the emission, $\Delta f = 40$ Hz, and using $\theta_{kv} = 110^\circ$, this equation then provides a second independent estimate of the minimum wavelength, which works out to be $\lambda_{\min} = 0.70$ km. The estimated minimum wavelength is again much longer than the effective length of the Voyager dipole antenna. The corresponding minimum phase velocity of the plasma oscillations is then $f_p \lambda_{\min} = 2103 \text{ km s}^{-1}$, again greater than the electron thermal velocity, both consistent with the results of the previous paragraph.

4. Origin of the Emission Line

In the initial report of the emission line by Ocker et al. (2021), the origin of the emission was not well-understood. At that time, we thought that the emission might be thermally driven because of the close similarity to a very weak narrowband emission known as “Quasi-Thermal Noise” (QTN) that is commonly observed by plasma wave instruments in the solar wind (Meyer-Vernet 1979; Meyer-Vernet & Perche 1989; Meyer-Vernet et al. 2017). Whether the emission line is in fact QTN noise is an open question. The primary difficulty is that, according to the QTN theory, the plasma emission line can only be detected if the electric dipole antenna length is greater than the Debye length. Although the Voyager PWS electric antenna has a V-shaped configuration that does not correspond exactly to the simple linear dipole antenna envisioned by Meyer-Vernet et al., the effective length of the PWS electric dipole antenna, 7.1 m, is substantially less than the Debye length, which has been estimated to be about

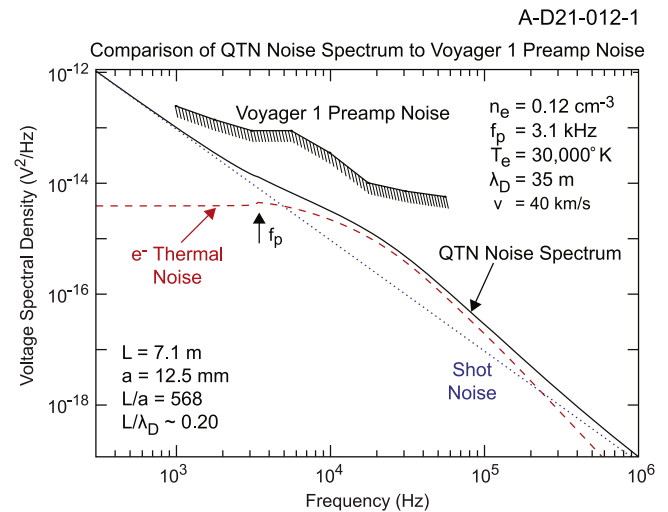


Figure 4. A comparison of the threshold sensitivity of the Voyager 1 PWS preamplifier to the QTN voltage spectrum predicted at the terminals of the PWS electric dipole antenna using the model of Meyer-Vernet & Perche (1989) and the currently accepted interstellar plasma parameters: $n_e = 0.12 \text{ cm}^{-3}$ and $T_e = 30,000 \text{ K}$ for a Maxwellian electron velocity distribution. The “Shot Noise” is the noise due to electrons striking the electric dipole antenna and is proportionate to the surface area of the antenna. The dimensions in the lower left-hand corner are the effective length, L , and diameter, a , of the PWS electric dipole antenna.

35 m. Thus, for an equilibrium thermal (Maxwellian) electron velocity distribution, the QTN emission should not be observed. This difficulty is dramatically illustrated in Figure 4, which shows the computed QTN voltage spectrum that should be detected by the PWS electric dipole using the nominal plasma parameters that exist in the VLISM, (electron density of $n_e = 0.12 \text{ cm}^{-3}$ and temperature of $T_e = 30,000 \text{ K}$). As can be seen, for the Voyager antenna dimensions and the nominal plasma parameters in the VLISM, the predicted QTN voltage spectrum shows no evidence of a narrowband emission line at the electron plasma frequency.

Also, the QTN spectrum is well below the PWS preamplifier sensitivity, which is shown overplotted in Figure 4.

That essentially no emission line is predicted for the current interstellar plasma parameter using a Maxwellian electron velocity distribution is consistent with our understanding of the physics of the QTN emission mechanism and our evidence that the phase velocity of the plasma oscillations is much greater than the electron thermal velocity. In the QTN theory, the emission line is linked to the real part of the impedance, $Z = R + iX$, of the electric antenna. The resistance, R , is caused by the dissipation of damped plasma oscillations excited as part of the impedance measurement process, which involves driving an oscillating current of various frequencies into the antenna and measuring the resulting voltage across the terminals as a function of frequency. If the wavelength of the resulting plasma oscillations is much longer than the length of the antenna, as argued in the previous section, then there can be no significant far-field excitation of the electron plasma oscillations by the injected current, no resistance, R , and no possibility of a thermally excited emission line associated with the resistive part of the impedance.

5. Discussion and Conclusions

If the emission line cannot be explained by the QTN theory for a Maxwellian thermal plasma, what are some possibilities for understanding the emission line within the parameters of the QTN theory? We list three possibilities:

1. Reevaluate the interstellar plasma parameters to see if the electron temperature might be significantly lower than the 30,000 K. This would reduce the Debye length and make the QTN theory more viable.
2. Modify the QTN theory to include the effect of suprathermal electrons. This would be consistent with our evidence that the primary interactions with the antenna occur at velocities well above the electron thermal velocity.
3. Consider the possibility that the emission line is not excited by fluctuations due to thermal (Brownian-motion-like) effects, but rather are due to fluctuations caused by the cascade of interstellar turbulence down to spatial scales on the order of kilometers.

Next, we discuss the possible merits of these three possibilities. Because the QTN theory depends so critically on the ratio of the electric antenna length to the Debye length, it is useful to consider how well we know the interstellar plasma parameters. Two parameters control the Debye length, the electron density, n_e , and the electron temperature, T_e . Of these, the electron density is believed to be very well-determined, because it is derived from the frequency of electron plasma oscillations, which can be measured very accurately, typically to a few percent. The situation with respect to the electron temperature is much less certain. The temperature range, 30,000–50,000 K, reported by Richardson et al. (2019) is based on measurements of interstellar ions detected by the Voyager 2 PLS, and is not based on electron measurements. In fact, no measurements of low-energy, <10 keV, electrons are currently available in the VLISM from Voyager (Bridge et al. 1977; Krimigis 1977; Richardson et al. 2019). Our use of $T_e = 30,000$ K to estimate the Debye length assumes that the electrons are in thermal equilibrium with the ions. Since agreement with the QTN theory can only be improved by decreasing the electron temperature (hence the Debye length), we need to consider to what extent the electron temperature could be substantially lower. Based on Ulysses-IBEX measurements, a

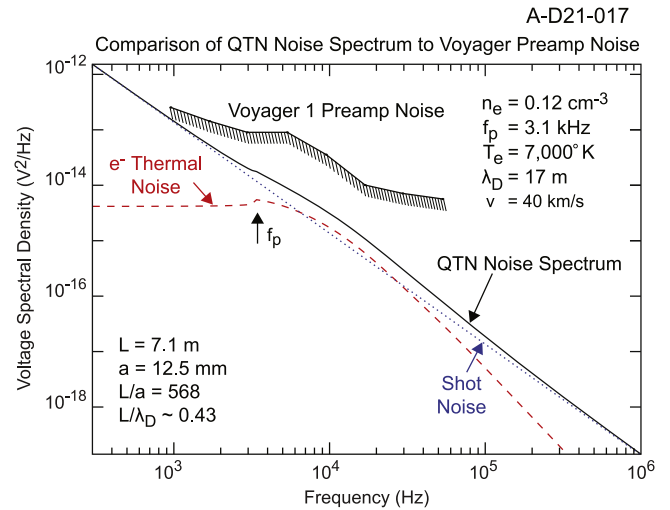


Figure 5. The computed QTN voltage spectral density that would be expected at the terminals of the Voyager 1 electric dipole antenna for a Maxwellian electron distribution with a density of 0.12 cm^{-3} and a temperature of 7000 K. Although a slight peak can be seen in the electron thermal noise at f_p , this peak is far below the noise level of the Voyager 1 preamplifier noise level and would not be detected as an emission line.

consensus has been reached that the plasma temperature in the local interstellar medium is not less than about 7000 K (McComas et al. 2015). If we use 7000 K as the electron temperature for a Maxwellian electron velocity distribution, we can compute the voltage spectrum that would be observed by the Voyager PWS electric antenna according to the QTN theory. This spectrum is shown in Figure 5. As can be seen, there is no evidence of an emission at the plasma frequency that is even remotely close to the noise level of the Voyager PWS preamplifier. We conclude that there is no variation of the currently known interstellar parameters that could lead to a detectable thermal emission line at the electron plasma frequency for a purely Maxwellian plasma.

Because our earlier studies indicated that the primary interactions responsible for the plasma emission line occur at phase velocities well above the electron thermal velocity, we decided next to investigate the effects of suprathermal electrons on the QTN voltage spectrum. Fortunately, several researchers have already considered such suprathermal effects; see Chateau & Meyer-Vernet (1989, 1991), Meyer-Vernet & Perche (1989), Le Chat et al. (2009), Yoon (2014), and more recently, Meyer-Vernet et al. (2017). The technique they pioneered was to use a kappa velocity distribution function to represent a high-energy tail of an otherwise thermal (Maxwellian) velocity distribution. A convenient form for the “kappa” velocity distribution function is given by Le Chat et al. (2009):

$$f_{\kappa}(v) = \frac{\Gamma(\kappa + 1)}{(\pi\kappa)^{3/2} v_0^3 \Gamma(\kappa - 1/2) (1 + v^2/\kappa v_0^2)^{\kappa+1}}, \quad (3)$$

where the kappa parameter, κ , is a positive constant that can be varied anywhere from $3/2$ to infinity, $\Gamma(x)$ is the gamma function, v is the speed in three dimensions, $v = (v_x^2 + v_y^2 + v_z^2)^{1/2}$, v_0 is the most probable speed defined by

$$v_0 = \sqrt{\frac{2\kappa - 3}{\kappa} \frac{k_B T_{\kappa}}{m_e}}, \quad (4)$$

k_B is Boltzmann’s constant, m_e is the electron mass, and T_{κ} is the temperature of the kappa distribution. As κ approaches

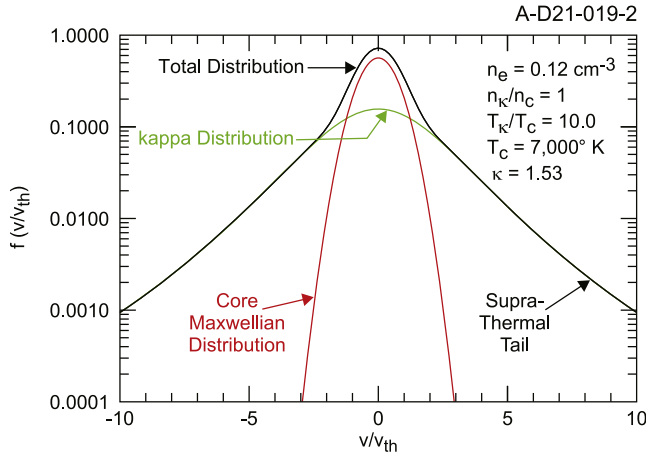


Figure 6. The core Maxwellian and kappa distribution used to simulate a suprathermal high-energy tail in the calculation of the resulting QTN voltage spectrum in Figure 7.

infinity, $f_\kappa(v)$ becomes a Maxwellian velocity distribution, and as κ becomes small, the distribution function develops a power-law tail. Note that the kappa distribution is undefined for $\kappa < 3/2$. For a kappa distribution, the Debye length becomes dependent on κ . The shielding length is then given by Bryant (1996)

$$\lambda_\kappa = \lambda_D \left[\frac{\kappa - 3/2}{\kappa - 1/2} \right]^{1/2}, \quad (5)$$

where λ_D is the (Maxwellian) Debye length. Note that, as κ approaches infinity, $\lambda_\kappa \rightarrow \lambda_D$, and as κ approaches $3/2$, the Debye length goes to zero, indicating no shielding at all.

To investigate the effects of an electron power-law tail on the QTN voltage spectrum, we used a series of distribution functions consisting of a core Maxwellian with a temperature T_c , and a kappa distribution with a temperature T_κ . The objective was to investigate the QTN voltage spectrum as κ is made smaller, approaching $3/2$, in order to produce a high-energy tail. We integrated the antenna current distribution (e.g., Meyer-Vernet & Perche 1989; Meyer-Vernet et al. 2017) assuming a dipole antenna geometry at frequencies $\Delta f/f$ from a few percent down to $\Delta f/f \sim 1\%$ near the plasma frequency using Mathematica with adaptive precision. Lacking any other experimental guidance, we set the electron density of the kappa distribution equal to the electron density of the core Maxwellian, $n_\kappa = n_c$, and the temperature of the kappa distribution to ten times that of the Maxwellian, $T_\kappa = 10T_c$. The resulting distribution function is shown in Figure 6. By experimenting with various values of kappa, we discovered that, as κ approaches $3/2$ from above, the voltage spectral density of the QTN noise began to develop a very distinct narrowband peak at f_p . A representative QTN voltage spectral density spectrum for $\kappa = 1.53$ is shown in Figure 7. From such experimentation, we conclude that, if a sufficiently strong electron high-energy tail exists in the VLISM medium, the QTN theory could produce a narrowband emission line that extends above the Voyager PWS preamp noise level, thereby potentially explaining the very weak emission line reported by Ocker et al. (2021). This trend for a narrowband emission to develop for small κ has been noted before by Le Chat et al. (2009). The reason for this positive development appears to be that, as κ becomes small, the high-energy tail causes the effective Debye length to decrease significantly, thereby increasing the coupling of electrostatic

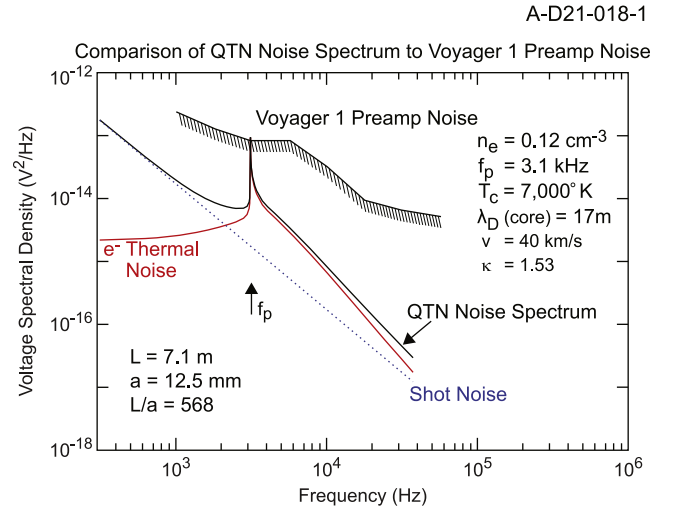


Figure 7. The computed QTN voltage spectral density that would be expected at the terminals of the Voyager 1 electric dipole antenna for the Maxwellian/kappa electron distribution function shown in Figure 6. The presence of a high-energy tail in the kappa distribution ($\kappa = 1.53$) leads to a sharp, well-defined emission at f_p that was not in the comparable plot in Figure 5 for a purely Maxwellian electron velocity distribution. The presence of this emission is attributed to the much better coupling of thermal or turbulent-driven electrostatic potential fluctuations in the plasma to the antenna due to the greatly reduced Debye length associated with the small kappa value ($\kappa = 1.53$).

potential fluctuations in the plasma to the electric dipole antenna. This effect essentially negates the often-stated condition that the effective length of the dipole antenna must be much greater than the Debye length for the QTN emission line to be observed. Since our calculation includes both a kappa distribution and a Maxwellian distribution of equal density, the effective Debye length will be intermediate between these two extremes.

From the above discussion, it is apparent that the QTN theory can potentially account for the weak emission line observed by Voyager 1 if a sufficiently dense high-energy tail is present in the plasma. Whether such a high-energy tail is present in the VLISM cannot currently be determined because Voyager does not have adequate instrumentation to detect such suprathermal electrons. So, in the absence of adequate measurements, the question then becomes whether there exists a known mechanism for generating such a suprathermal electron distribution in the VLISM. This is not a minor issue, because for the kappa distribution that produced the narrowband emission in Figure 7, the total energy of the suprathermal electron population is ten times that in the core Maxwellian distribution. One such mechanism that could lead to such energization is by lower-hybrid waves driven by pickup ions as has been suggested by Cairns & Zank (2002). Other similar mechanisms may be important.

Irrespective of how the high-energy electron population is produced, or if it exists at all, one can pose the further question: how do we know the fluctuations that drive the narrowband emission are caused by statistical (Brownian-motion-like) variations in the phase-space density of the high-energy tail? The answer is that we do not. There could very well be other forces that drive these fluctuations. For example, Lee & Lee (2019) have made measurements claiming that the cascade of the well-known power-law interstellar turbulence spectrum extends down to spatial scales on the order of kilometers, or even 50 m, with density fluctuations on spatial scales that we estimate could be as large as $\Delta n/n \sim 1\%$. We should give serious consideration to the possibility that such turbulent

fluctuations could drive the narrowband emission line recently discovered by Voyager 1.

We thank John Richardson and John Belcher of MIT for their comments on the capabilities of the Voyager Plasma (PLS) instrument. We also thank William Thompson, Lan Jain, Jeewoo Park, and Frederico Fraternali for their efforts estimating the angle between the interstellar flow velocity and the magnetic field direction at Voyager 1 around 2020 January 1. The research at the University of Iowa was supported by NASA through Contract 1622510 with the Jet Propulsion Laboratory. The research by L.F.B. was supported by NASA via contract 80GSFC19C0012, the research by N.V.P. was supported by NASA grant 80NSSC18K1649, and the research by D.B.B. was supported by the NASA Voyager Project. The Voyager PWS data are regularly archived with the Planetary Data System at https://pds-ppi.igpp.ucla.edu/search/view/?id=pds://PPI/VG1-J_S_SS-PWS-1-EDR-WFRM-60MS-V1.0 and at CDA-Web at <https://cdaweb.gsfc.nasa.gov>.

ORCID iDs

D. A. Gurnett  <https://orcid.org/0000-0003-2403-0282>
 W. S. Kurth  <https://orcid.org/0000-0002-5471-6202>
 L. F. Burlaga  <https://orcid.org/0000-0002-5569-1553>
 N. V. Pogorelov  <https://orcid.org/0000-0002-6409-2392>
 M. Pulupa  <https://orcid.org/0000-0002-1573-7457>
 S. D. Bale  <https://orcid.org/0000-0002-1989-3596>

References

Ajello, J. M., Steward, A. I., Thomas, G. E., & Garps, A. 1987, *ApJ*, **317**, 964
 Axford, W. I. 1990, in *Physics of the Outer Heliosphere*, ed. S. Gredzielski & D. E. Page (Oxford: Pergamon), 7

Bridge, H. S., Belcher, J. W., Butler, R. J., et al. 1977, *SSRv*, **21**, 259
 Bryant, D. A. 1996, *JPIPh*, **56**, 87
 Burlaga, L. F., Kurth, W. S., Gurnett, D. A., et al. 2021, *ApJ*, **911**, 6
 Burlaga, L. F., Ness, N. F., Berdichevsky, D. B., et al. 2019, *NatAs*, **3**, 1007
 Burlaga, L. F., Ness, N. F., & Stone, E. C. 2013, *Sci*, **341**, 147
 Cairns, I. H., & Zank, G. P. 2002, *GeoRL*, **29**, 471
 Chateau, Y. F., & Meyer-Vernet, N. 1989, *JGRA*, **94**, 15407
 Chateau, Y. F., & Meyer-Vernet, N. 1991, *JGRD*, **96**, 5825
 Davis, L. E., Jr. 1955, *PhRv*, **100**, 1440
 Filbert, P. C., & Kellogg, P. J. 1979, *JGRA*, **84**, 1369
 Frisch, P. C., Redfield, S., & Slavin, J. D. 2011, *ARA&A*, **49**, 237
 Gurnett, D. A., & Bhattacharjee, A. 2017, *Introduction to Plasma Physics* (2nd edn.; Cambridge: Cambridge Univ. Press), 10
 Gurnett, D. A., & Kurth, W. S. 2019, *NatAs*, **3**, 1024
 Gurnett, D. A., Kurth, W. S., Burlaga, L. F., & Ness, N. F. 2013, *Sci*, **341**, 1489
 Kim, T. M., Pogorelov, N. V., & Burlaga, L. F. 2017, *ApJL*, **843**, L32
 Krimigis, S. M. 1977, *SSRv*, **21**, 329
 Krimigis, S. M., Decker, R. B., Roelof, E. C., et al. 2013, *Sci*, **341**, 144
 Krimigis, S. M., Decker, R. B., Roelof, E. C., et al. 2019, *NatAs*, **3**, 997
 Le Chat, G., Issautier, K., Meyer-Vernet, N., et al. 2009, *PhPl*, **16**, 102903
 Lee, K. H., & Lee, L. C. 2019, *NatAs*, **3**, 154
 McComas, D. J., Bzowski, M., Frisch, P., et al. 2015, *ApJ*, **801**, 28
 McComas, D. J., Funsten, H. O., Fuselier, S. A., et al. 2011, *GeoRL*, **38**, L18101
 Meyer-Vernet, N. 1979, *JGRA*, **84**, 5373
 Meyer-Vernet, N., Issautier, K., & Moncuquet, M. 2017, *JGRA*, **122**, 7925
 Meyer-Vernet, N., & Perche, C. 1989, *JGRA*, **94**, 2405
 Ocker, S. K., Cordes, J. M., Chatterjee, S., et al. 2021, *NatAs*, **5**, 761
 Parker, E. N. 1963, *Interplanetary Dynamical Processes* (New York: Interscience Publishers)
 Pogorelov, N. V., Heerikhuisen, J., Roytershteyn, V., et al. 2017, *ApJ*, **845**, 9
 Richardson, J. D., Belcher, J. W., Garcia-Galindo, P., & Burlaga, L. F. 2019, *NatAs*, **3**, 1019
 Stone, E. C., Cummings, A. C., Heikkila, B. C., & Lai, N. 2019, *NatAs*, **3**, 1013
 Stone, E. C., Cummings, A. C., McDonald, F. B., et al. 2013, *Sci*, **341**, 150
 Tonks, L., & Langmuir, I. 1929, *PhRv*, **33**, 195
 Yoon, P. 2014, *JGRA*, **119**, 7074
 Zank, G. P. 2015, *ARA&A*, **53**, 449